ORIGINAL ARTICLE

AI-AIDED VOLUMETRIC ROOT RESORPTION ASSESSMENT FOLLOWING PERSONALIZED FORCES IN ORTHODONTICS: PRELIMINARY RESULTS OF A RANDOMIZED CLINICAL TRIAL

NAVARRO-FRAILE ESTRELLA[a], DEHESA-SANTOS ALEXANDRA[a], CHEN YUN[a], JUAN CARLOS PALMA-FERNÁNDEZ[a], AND IGLESIAS-LINARES ALEJANDRO[a,b]

[a]School of Dentistry, Complutense University of Madrid, Madrid, Spain
[b]BIOCRAN, Craniofacial Biology and Orthodontics Research Group, School of Dentistry, Complutense University of Madrid, Madrid, Spain

Introduction
External apical root resorption (EARR) is an undesirable loss of hard tissues of the tooth root frequently affecting to the maxillary incisors. The magnitude of orthodontic forces is a major treatment-related factor associated with EARR occurrence in orthodontics. The primary aim of the present randomized clinical trial was (i) to quantify the impact of a sequence of personalized force archwires on EARR compared to the conventional standard of care and (ii) compare the 3D-quantification of EARR using two quantification methods (manual or automated AI-aided segmentation).

Material and Methods
A superiority two arms-parallel-randomized clinical trial (RCT) was conducted to quantify the EARR of two regime forces [CONSORT-guidelines]. A total of 18/43 patients were randomly assigned [block-size: 4] to *Control Group* [Ni-Ti archwires sequence] or *Experimental Group* [selective *individualized* force archwires]. After 142 days sectorial CBCT were obtained; upper incisors were segmented manually and with AI and the volume/length of root quantified. Method error/descriptive statistics (mean; SD; range) and Student *t*-test were used to assess the differences between groups (*Post hoc* adjustment for confounders [95% CI; $P < .05$]).

Results
The total root volume loss detected by AI was 2.44 ± 6.59 mm^3 / 2.42 ± 4.75 mm^3 ($P > .05$) and the mean root length loss was 0.20 ± 0.23mm/0.42 ± 0.43 mm ($P = .045$) for control/test group, respectively. Despite length loss showed similar changes when it was quantified with both methods, manual and automatic segmentations ($P > .05$), differences are observed at volume loss. The results demonstrated greater volume loss detection with manual segmentation than with AI-aided segmentation at the global level, volume by thirds, and 4 mm from the apex. However, as we approached apically, the differences equalized and even diminished, resulting in a greater loss with automatic segmentation 1 mm from the apex in the EG ($P = .011$).

Conclusions
A non direct-force-dependent effect over EARR (6 months) was observed. Individualized force induces slightly higher root resorption at the apical third at 1-2 mm.

CORRESPONDING AUTHOR
Alejandro Iglesias-Linares, School of Dentistry, BIOCRAN-Craniofacial Biology and Orthodontics Research Group, Complutense University of Madrid, Pza. Ramón y Cajal, s/n. Ciudad Universitaria, Madrid, 28040 Spain.
E-mail: Aleigl01@ucm.es

KEYWORDS
Resorption, CBCT, RCT, AI

Conflict of interest: The authors have no actual or potential conflicts of interest.

Source of funding: DECO Department. School of Dentistry. University Complutense of Madrid.

Received 29 August 2024; revised 31 December 2024; accepted 16 January 2025

J Evid Base Dent Pract 2025: [102095]

1532-3382/$36.00

doi: https://doi.org/10.1016/j.jebdp.2025.102095

INTRODUCTION

External apical root resorption (EARR) is defined as the undesirable loss of hard tissues of the tooth root, such as dentin and cement.[1] High-magnitude force levels (>225 g) and particular orthodontic movements (ie, intrusion or buccal tipping) are associated with an increased risk of root resorption. 2,3 Accurate EARR detection has been challenging in orthodontics because of the inherent limitations of routine two-dimensional (2D) records, ie, image distortion, underestimation, and questionable prediction.[4,5] The incorporation of three-dimensional (3D) radiological images, including cone-beam computed tomography (CBCT), has overcome some of these 2D limitations.[6-9] However, there is still a scarcity of studies on EARR predisposition based on 3D radiological records[10] and on randomized controlled clinical studies.[11-16]

EARR occurs in 19%-93% orthodontically treated patients,[8] and its etiology is considered multifactorial. Several patient-related factors (individual susceptibility or genetic predisposition) and treatment-related factors (the appropriate biomechanical forces used during orthodontic treatment) may influence the occurrence of EARR during orthodontic treatment.[17,18]

The maxillary incisors are most commonly affected by EARR,[8,19] and the magnitude of orthodontic forces and the duration of orthodontic treatment are the two major treatment-related factors associated with EARR occurrence in orthodontics.[2,6,20-22] Related to the time factor, some studies have reported that the severity of apical root resorption in the upper incisors could be predicted in the first 6 months of orthodontic treatment.[23,24] This initial period often involves a greater amount of tooth movement during the leveling and alignment phases.[3,5] In the last few years, multiforce archwires, which provide selective forces according to the type of tooth in the initial stages of treatment, have been introduced in the market. In addition to the different force zones, these arches enable alignment, levelling, and torque expression simultaneously during the early stages of orthodontic treatment, with the working phase commencing prior to that when traditional arches are utilised.[25] Moreover, although the root volume and crown-root ratio vary dramatically from the anterior to posterior teeth,[26] conventional initial orthodontic archwires, commonly used with fixed appliances, exert an identical magnitude of force on the anterior and posterior teeth, independent of these root volumetric differences.[27,28] Several *in vitro* studies have compared the mechanical properties of standardized Ni-Ti archwires with those featuring various force zones.[25,29,30] Nevertheless, to the best of our knowledge, no *in vivo* studies have quantified the impact of selective personalized forces on EARR during the first phase of orthodontic treatment.

Accurate radiological diagnosis of EARR remains a challenge in current orthodontic practice. Despite the overall superiority of CBCT records in terms of diagnostic precision compared to 2D radiographic methods,[31] one of the most challenging goals is the reduction in both time consumption and the incidence of misdiagnosis based on observer dependence.[32,33] CBCT image segmentation, required for precise EARR quantification, is considered a laborious process owing to different factors, such as the similarity of densities of surrounding tissues, image resolution, or the presence of different artifacts, which may alter the record quality. According to different segmentation methods, the process has traditionally been partially or totally operator dependent (semi-automatic or manual methods, respectively). [34,35] A semi-automatic process that creates a three-dimensional (3D) surface based on the thresholding tool of open-source 3D software requires manual refinement to complete the segmentation. On the other hand, the manual method is a longer process that involves clinician intervention during the entire procedure to improve the surface anatomy and carefully adjust areas of distortion by artefacts, such as orthodontic brackets.

To overcome these limitations involving collaboration of the clinician, the incorporation of artificial intelligence (AI)-aided digital processes (fully automatic segmentation) has gradually become useful in several time-consuming tasks to improve and automate the process of anatomical structure segmentation based on cone-beam computed tomography images.[36] AI encompasses various models that can be used to solve a range of problems, from predictive analysis to image recognition.[37] Machine learning (ML) is a broad subfield of AI that uses computational methods and data for training. Within ML, there is a specialized subset called deep learning (DL), which uses neural networks with multiple layers to automatically extract features and learn from complex datasets. A convolutional neural network is a specialised type of DL model designed for image data with medical applications, such as radiographic analysis, segmentation, and interpretation.

We hypothesized that there would be no difference in the occurrence of EARR between orthodontic multiforce archwires and conventional Ni-Ti archwires during the initial stages of orthodontic treatment. Hence, the primary aim of the present randomized clinical trial was (i) to quantify the impact of a sequence of personalized force archwires on EARR compared to the conventional standard of care during the leveling and alignment phases and (ii) compare the 3D-quantification of EARR using two quantification methods (manual or automated AI segmentation).

Figure 1. Trial design.

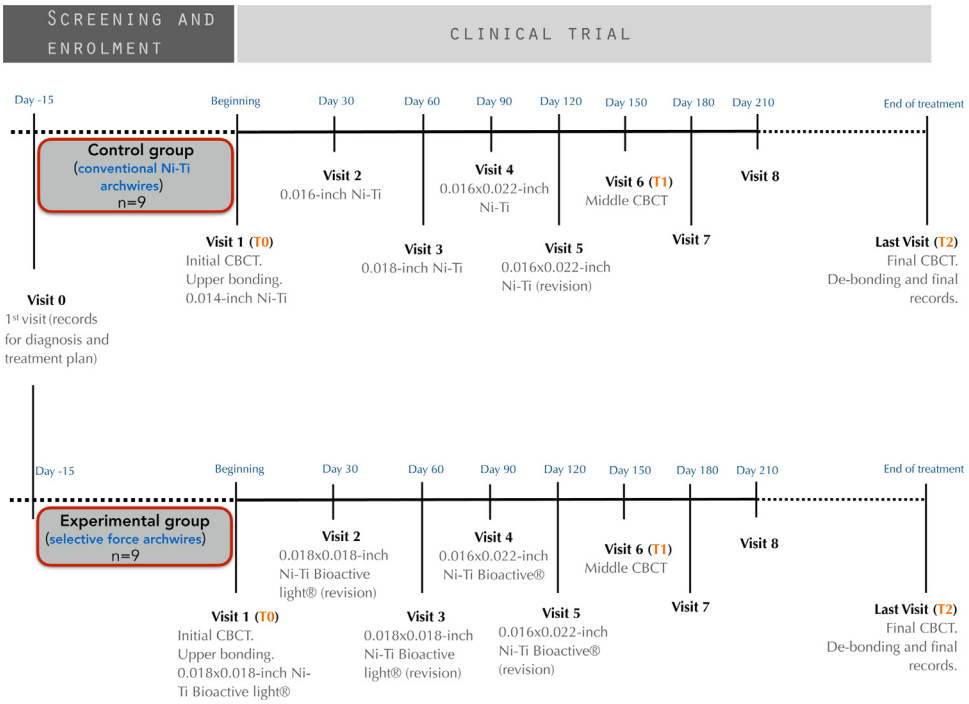

MATERIALS AND METHODS

Ethical Statement and Protocol Registration

This clinical trial followed the requirements of the Helsinki Declaration,[38] was approved by the Institutional Ethical Review Board (21/003-EC_P) and the Institutional Local Review Board (*URI+i: 51-100521*), and was registered in the Clinical Trials database (*NCT04870463*).

Clinical Trial Design and Setting

The present study was designed as a two-arm, parallel-group, randomized controlled clinical trial, with a 1:1 allocation of patients, to evaluate the superiority of experimental individualized forces (experimental group [EG]) compared with the *gold standard* sequence of reference forces (control group [CG]). The trial was designed according to the CONSORT guidelines and was conducted in the Orthodontic Department of the School of Dentistry of Complutense University (UCM), Madrid, Spain. A detailed description of the trial design is presented in Figure 1. (*Trial registration:* NCT04870463 *Registered 3 may 2021*, https://classic.clinicaltrials.gov/ct2/show/NCT04870463)

Participants

Sampling of consecutive cases was performed during participants' enrollment in the trial. Patients requiring orthodontic treatment were asked to participate. Participant recruitment and screening were conducted by researchers E.N.F. and A.D.S. Accordingly, those who met the eligibility criteria (*Supplementary Table 1*) were invited to participate in the study. Written informed consent was obtained from all participants after they received comprehensive oral and written information about the project protocol prior to formal enrollment. The baseline characteristics of the participants are summarized in Table 1, and a CONSORT flowchart of the trial is shown in Figure 2.

Sample Size Estimation

The sample size was estimated based on the preliminary results obtained from representative cohorts under similar inclusion criteria.[39] Apical volume loss was considered as the primary outcome. Considering a mean apical volume loss in the control group (1.47 ± 1.13 mm^3) and in the experimental group (2.82 ± 1.47 mm^3), an effect size of 1.029695 [Hedges' g = (2.82-1.47) / 1.311068] was calculated (under an 80% power and significance level of 95% [$\alpha = .05$]). Taking the tooth as a sample unit and considering a 30% dropout rate, a minimum sample of 26 was required.

Sequence Generation and Concealment, Randomization, and Blinding Procedures

A block randomization scheme was used to ensure a balance (1:1) between the control and experimental groups.

Table 1. Baseline characteristics of the groups.

	Control ($n = 9$) Mean ± SD	Experimental ($n = 9$) Mean ± SD	*P* value
Age (y)	27.4 ± 18.7	26.7 ± 15.0	.931
Gender *n* (%)	5 (55.6%) female	5 (55.6%) female	1.000
	4 (44.4%) male	4 (44.4%) male	
Treatment duration (d)	140.0 ± 3.6	143.9 ± 5.3	.113
Extractions (n)	0	2	-
Malocclusion (*n*)			1.000
Class I	3 (33.3%)	3 (33.3%)	
Class II	5 (55.6%)	5 (55.6%)	
Class III	1 (11.1%)	1 (11.1%)	
SD: standard deviation.			

Figure 2. CONSORT flowchart.

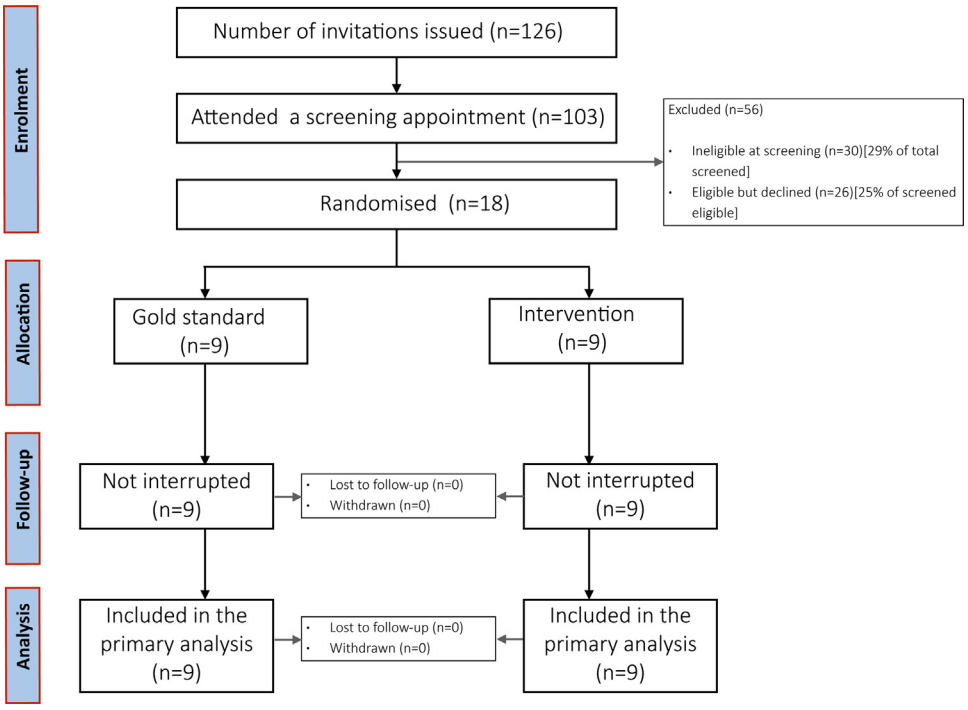

The patients were allocated to six blocks of four each (fixed size). The main operator generated a random table of numbers using the online tool ⟨13:italic⟩https://www.randomizer.org⟨/13:italic⟩ and then concealed it from view. Twenty sets of 20 numbers were used to determine the selection order of the blocks by choosing numbers from one to six in the sequence.[40] This randomization scheme was developed by one of the research assistants (A.D.S. or Y.C.), who was unfamiliar with the need for treatment of each patient and unknown to the main operator (E.N.F) until the day of arch placement. In addition, the examiner was blinded to the measurement performance. The parents, participants, and the rest of the research team were blinded to the allocation.

Interventions

The participants were randomly allocated to one of two treatment strategies: *i)* selective forces (EG) or *ii) gold standard* of care with no individualized forces (CG), both provided by a single experienced orthodontist (E.N.F.) (Figure 1).

Before starting the treatment, a complete study of each patient was conducted, which included photographs, radiographs, intraoral scans, clinical exploration, and discussions with the research team to elaborate the treatment plan. Participants attended were treated with the orthodontic preadjusted 3 M Unitek® (Victory Series™ conventional-ligating brackets, slot 0.18″), and all wires were tied with steel ligatures.

Gold standard of care was provided following a protocol of arches sequence: 0.014-inch super-elastic Ni-Ti, 0.016-inch super-elastic Ni-Ti, 0.018-inch super-elastic Ni-Ti and 0.016 × 0.022-inch super-elastic Ni-Ti (3M Unitek®, United States). Each archwire remained in the upper arch for 28 ± 7 days, except for the rectangular wire, which remained for 56 days. Meanwhile, experimental group protocol followed: 0.018 × 0.018-inch Ni-Ti Bioactive light® and 0.016 × 0.022-inch Ni-Ti Bioactive® (Tomy®, Japan). In this group, the 0.018 × 0.018 arch remained for 84 days and the 0.016 × 0.022 arch remained for 56 days until the alignment and leveling phases were completed. The endpoint of the trial was settled at 141.9 ± 4.9 days in both groups (Figure 1). All subjects were scanned on each appointment with the TRIOS 3shape scan to calculate the amount of maxillary dental crowding.

Sectorial CBCT Records Acquisition

Sectorial CBCT scans were acquired at the beginning of treatment (T0) and after 5 months (T1) (142 ± 5 days). All scans were made using a standardized radiological protocol with Carestream cone beam (Carestream Heath Inc, model CS93000), and the scanning parameters were as follow: 5 × 5 FOV with a voxel size of 0.09 mm, exposure parameters of 8 s, voltage 90 kV, and tube current of 10 mA. Examinations were made such that the four upper incisors were contained in one volume, and root resorption was assessed at T0-T1 time-interval in the EG and CG (Figure 3). All scans were saved in Digital Imaging and Communication in Medicine (DICOM) format.

External Root Resorption Quantification

The external root resorption (ERR) analysis consisted of digital tooth segmentation, Standard Tessellation Language (STL) file generation, and 3D ERR quantification, as detailed below.

Digital Segmentation

Tooth segmentation was performed using two methods: manual and automated AI segmentation.

Manual segmentation:

Primary data reconstruction was made through the DICOM images at each time-point uploaded onto a free-access software (3D Slicer® 4.11.20210226). First, sagittal cuts of each CBCT scan were made to segment each tooth into a separate DICOM file. Volume rendering of each tooth was then reconstructed as described in Figure 3A. The densities of teeth and surrounding tissues vary among individuals; therefore, a uniform threshold value could result in data loss for tooth tissues in some cases. Therefore, the threshold values in this study were set individually for each tooth, and the Hounsfield units (HU) ranged from 1700 to 2000. In addition, owing to incomplete tooth contours in some CBCT images, after initial automatic segmentation, further manual correction using the "paint" and "erase" tools was required to add certain missing areas or remove noise or unrelated parts to ensure tooth anatomy was preserved without surrounding structures. The segmentation outcome generated for each incisor was then saved as a virtual 3D model in STL file format.

Automated-AI Segmentation:

The DICOM images were individually imported to an AI based on a deep learning method and custom-made software (Diagnocat®), where all the teeth in a scan were automatically segmented (Figure 3B). Each generated tooth segment was then saved in the STL file format.

Volumetric 3D Assessment of the ERR

Once tooth segmentation was generated, it was imported to Geomagic Wrap software® (Geomagic, Cary, N.C.) for the quantification of ERR based on root length and volumetric changes. Following a modified version of a previously validated method,[15] each incisor was oriented with its incisal edge parallel to the floor. After defining the cervical plane at three points, the tooth was virtually cut, and the crown was separated from the root (Figure 4A). Once the root was isolated, the root length and volume were measured from the reference plane (cervical plane) to the root apex (Figure 4B).

Figure 3. (A) Volumetric reconstruction of an upper left central incisor after manual segmentation in three-dimensional views (axial, coronal and sagital slices). (B) Volumetric reconstruction after automated segmentation. (i) complete scan, (ii) area of interest of maxillary incisor region.

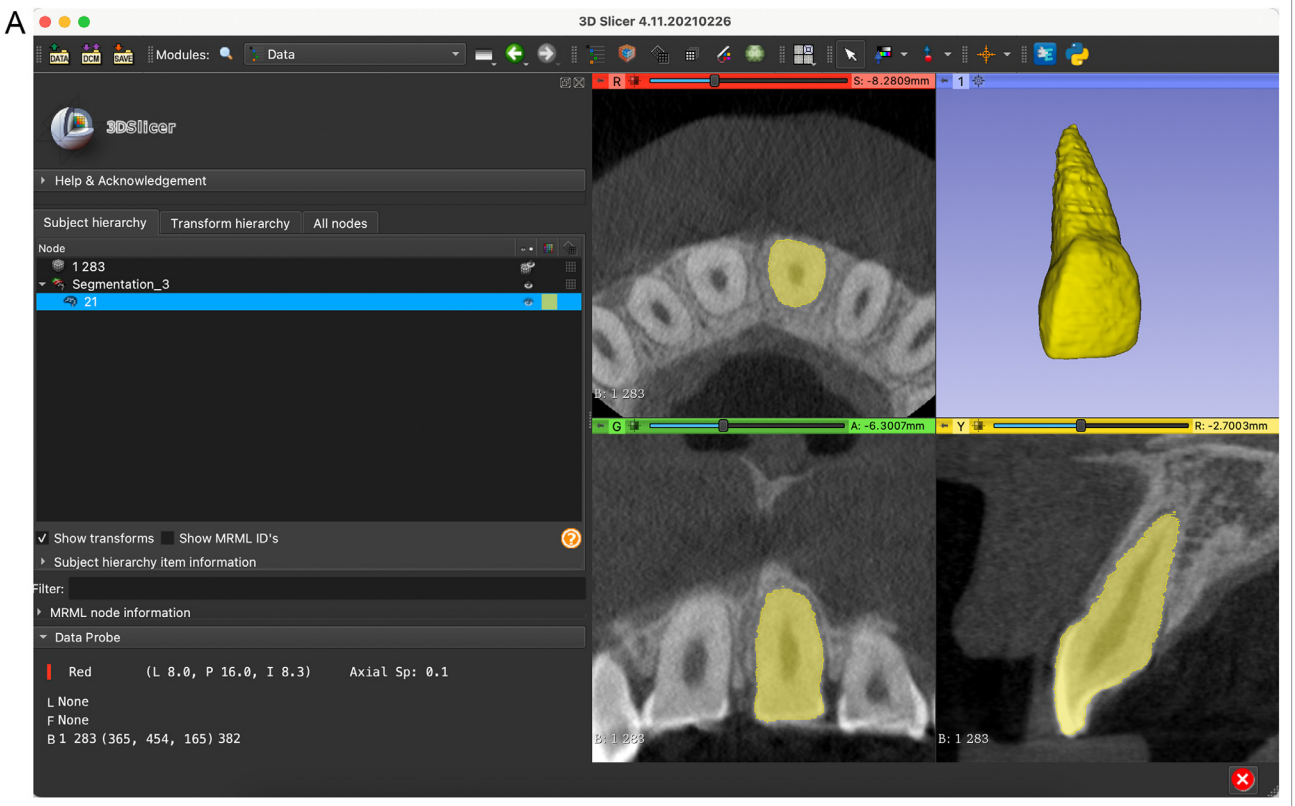

Figure 4. (A) Separation of the root from the crown through the cervical plane defined by 3 points at the cementoenamel junction (CEJ): 2 points on the labial side and 1 point on the palatal side. (B) Once root is segmented, both volume (i) and root length (ii) are computed. (C) Root is divided in three thirds (cervical, middle and apical) and the apical third is then cut at 1, 2 and 4 mm from the apex.

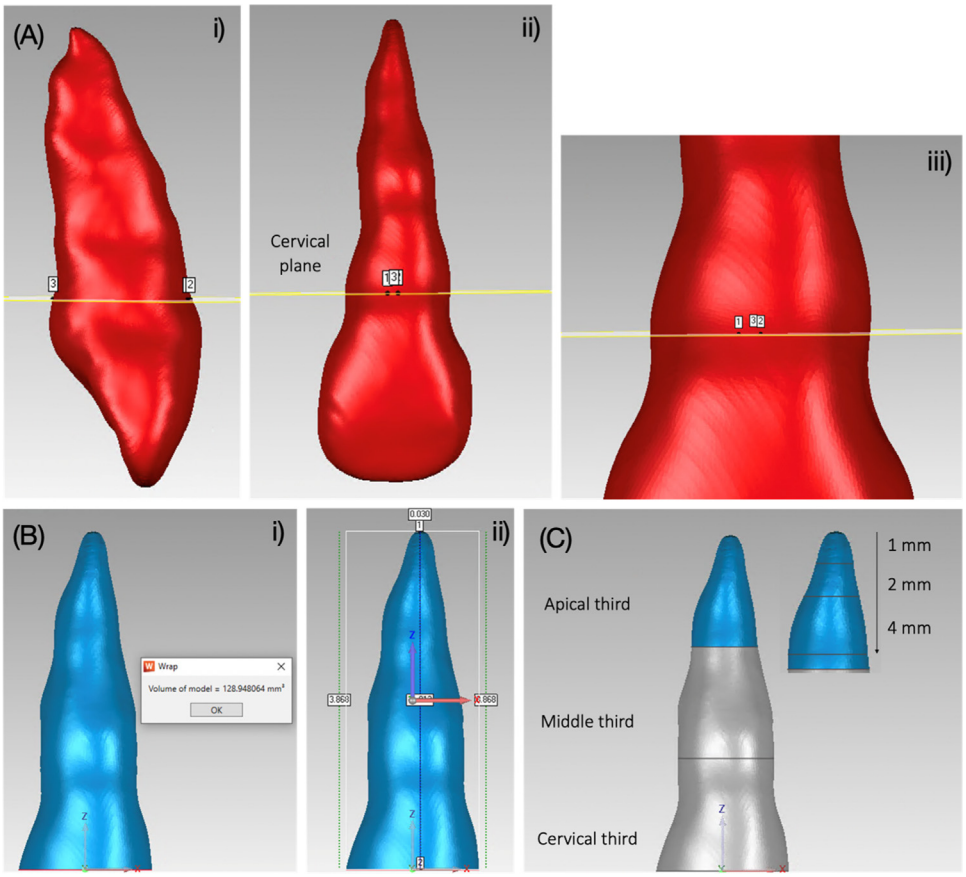

The root volume was then divided into three thirds (cervical, middle, and apical), and the volume of each third was calculated in mm^3 (Figure 4C). Apical volumes at 1, 2, and 4 mm from the apex were also calculated. This assessment was performed twice for each tooth after manual and automated segmentation. Finally, the root volume loss was calculated as the difference between the T0 and T1 root volumes.

Primary and Secondary Outcomes

The primary outcome was the *apical volume loss* (AVL), defined as the difference in the apical third volume between T0 and T1 (mm^3).[15]

The secondary outcomes measured included the *total root volume* quantification (TRV), *thirds root volume* quantification (CRV, MRV, and ARV), *volume at different heights in the apical third* (4 mm from the apex, 2 mm, and 1 mm), and *root length loss* (mm)(RLL), comparing the two different types of force applied between the groups. The results of two types of segmentation (manual and automated) were compared.

Statistical Analysis

Method Error and Accuracy

Pre-treatment (T0) and middle-treatment (T1) CBCTs scans of two patients (16 incisors in total) were randomly chosen and analyzed by two different investigators (E.N.F. and T.B.), and the measurements were repeated after 2 weeks using intraclass correlation with confidence intervals of 95%. Before the image interpretation, Dahlbergś formula was employed to evaluate the reliability of the measurements.

Association Analysis and Effect Size Adjustment

Normal distribution of the variables was checked using the Kolmogorov–Smirnov test. The results of this test confirmed that all the variables in the sample were normally distributed. Descriptive analyses were used to present the mean values

and standard deviations of root resorption (TRV, CRV, MRV, ARV, AVL, and RLL) for each group. A paired *t*-test was used to compare the pre- and post-treatment measurements in each group. ANOVA was used to compare the severity of root resorption between the two groups and the differences between the two segmentation processes (manual and AI). All analyses were conducted using generalized estimated equation models to consider the multiplicity of teeth per patient.

An exploratory multivariable regression analysis was performed to adjust the effect size of root resorption after adjusting for confounding factors (*age, sex, dental occlusion, and treatment duration*]. Statistical analysis was performed using SPSS software (version 26; IBM Corp, Armonk, NY, USA). The significance level was set at *P* value < .05.

RESULTS

Characteristics of the Included Patients and Method Error

A total of 103 participants attended a screening appointment, and after applying the eligibility criteria, 18 patients (69 upper incisors) were divided into two groups (CG and EG). Both groups were homogeneous in terms of sex distribution, and the mean age was 27.4 ± 18.7 years and 26.7 ± 15.0 years for CG and EG, respectively (Table 1). The overall treatment duration in both groups was 141.9 ± 4.9 days. No statistically significant differences in treatment force duration were observed between groups (CG: 140.0 ± 3.6 days and EG: 143.9 ± 5.3 days). The baseline characteristics of the participants, as described in Table 1, showed adequate homogeneity between the samples included in the comparative groups at the beginning of treatment (T0).

A total number of 36 CBCTs were analyzed. In addition, duplicate, manual, and automatic segmentation were performed on the 69 analyzed teeth. The intra- and intergroup comparison results for each group are summarized in Table 2 . Adequate reproducibility of the measurements was achieved with an ICC of 0.906 (confidence interval [CI] 0.8654-0.9351).

Root Loss Assessment After Personalized and Control Forces With Manual Segmentation

The results of root loss that occurred after the application of conventional or personalized forces under manual procedures are compiled in Table 2. The differences between the groups regarding the initial volume were slightly different in the middle and apical thirds ($P = .049$ and $P = .051$, respectively), where a slightly greater pre-treatment root volume was noted in the CG.

All parameters analyzed in each group showed significant differences between T0 and T1, indicating resorption in both groups ($P < .05$). However, when the two groups were compared, all changes were similar, without sufficient statistical evidence to consider significant differences between the groups ($P > .05$).

The influence of confounding factors on root resorption was detected in some patients (Table 3). Most importantly, the type of malocclusion and treatment duration influenced the ERR results.

Root Loss Assessment in Customized Forces and Controls With Automatic Segmentation

The CG and EG with automatic segmentation showed homogeneity at the beginning of the treatment (Table 2). Differences were observed in the apical third volume ($P = .042$). As with manual segmentation, the results showed a slightly greater volume in the middle and apical thirds in the CG than in the EG at the initiation of the study.

The changes between T0 and T1 in both the CG and EG are presented in detail in Table 2. Cervical and middle root volumes remained stable during treatment, and no significant differences were found between the groups ($P > .05$). However, root volume in the apical third decreased in both groups (1.14 ± 2.17 and 2.24 ± 2.60 mm^3 in CG and EG groups, respectively), with higher reduction experienced in the EG group ($P = .057$).

Total volume changed significantly in the EG group ($P = .019$) but not in the CG group ($P = .145$; 2.42 ± 4.75 mm^3 and 2.44 ± 6.59 mm^3 in EG and CG groups, respectively). However, these changes were not statistically significant when the groups were compared ($P = .992$).

When analyzed linearly, *root length* decreased significantly in both groups, but the loss was greater in the EG group (0.20 ± 0.23 and 0.42 ± 0.43 mm for CG and EG groups, respectively; $P = .060$).

The *volume loss* in the apical third increased significantly in both groups. However, at 1 and 2 mm from the apex, the variation in the EG group was significantly higher than in the CG group ($P = .040$ and $P = .020$ at 1 and 2 mm from the apex, respectively). At 4 mm, the *volume loss* increased slightly; however, when the groups were compared, no statistical differences were noted.

The influence of other confounding factors on root changes, when analyzed with the automatic segmentation procedure, appeared to be minimal. The only noticeable effect was observed in the *root length* variable, where a greater change was observed in younger patients ($P = .045$).

Comparison of 3D Loss Assessment Between Manual and Automatic Segmentation

The results demonstrated greater volume loss detection with manual segmentation than with AI-aided segmentation at

Table 2. Integroup comparison of root resorption at T0, T1 and the difference T0-T1, between manual and AI segmentation.

	Manual									AI									Manual vs AI	
	T0 (Baseline)			T1 (141.9 ±. 4.9)				T0-T1			T0 (Baseline)			T1 (141.9 ±. 4.9)				T0-T1			T0-T1	
	Control ($n = 36$)	Experimental ($n = 33$)		Control ($n = 36$)		Experimental ($n = 33$)		Control ($n = 36$)	Experimental ($n = 33$)		Control ($n = 36$)	Experimental ($n = 33$)		Control ($n = 36$)		Experimental ($n = 33$)		Control ($n = 36$)	Experimental ($n = 33$)		Control ($n = 36$)	Experimental ($n = 33$)
	Mean ± SD	Mean ± SD	*P* value	Mean ± SD	*P* value	Mean ± SD	*P* value	Mean ± SD	Mean ± SD	*P* value	Mean ± SD	Mean ± SD	*P* value	Mean ± SD	*P* value	Mean ± SD	*P* value	Mean ± SD	Mean ± SD	*P* value	*P* value	*P* value
All incisors																						
Root length (mm)	13.32 ± 0.91	12.59 ± 1.73	.199	13.02 ± 0.98	< .001*	12.15 ± 1.84	.001*	0.30 ± 0.37	0.45 ± 0.46	.303	12.99 ± 0.92	12.34 ± 1.74	.255	12.79 ± 0.95	< .001*	11.92 ± 1.81	< .001*	0.20 ± 0.23	0.42 ± 0.43	.060	.184	.686
Root volume (mm^3)	208.40 ± 44.30	181.52± 47.23	.081	200.18 ± 42.46	< .001*	175.47 ± 46.83	< .001*	8.22 ± 9.23	6.05 ± 4.76	.343	205.76 ± 45.66	182.26± 47.13	.128	203.32 ± 45.12	.154	179.84 ± 47.56	.019*	2.44 ± 6.59	2.42 ± 4.75	.992	<.001*	.001*
Cervical 1/3 volume (mm^3)	107.72 ± 23.68	98.06 ± 25.32	.213	105.31 ± 23.06	.025*	96.47 ± 25.43	.007*	2.41 ± 5.10	1.59 ± 2.94	.504	105.49 ± 24.21	97.60 ± 25.55	.318	104.86 ± 24.55	.513	97.36 ± 25.69	.610	0.63 ± 3.62	0.24 ± 2.00	.718	.264	.039*
Middle 1/3 volume (mm^3)	73.65 ± 16.11	61.91 ± 17.29	.049*	69.84 ± 14.57	< .001*	59.67 ± 17.05	.015*	3.81 ± 5.47	2.24 ± 4.45	.216	71.99 ± 15.91	61.54 ± 16.57	.061	71.33 ± 15.40	.302	61.29 ± 16.77	.645	0.67 ± 2.62	0.25 ± 2.39	.624	<.001*	.001*
Apical 1/3 volume (mm^3) (AVL)	27.79 ± 6.61	22.53 ± 8.00	.051	24.88 ± 6.56	< .001*	19.34 ± 6.53	< .001*	2.92 ± 2.43	3.19 ± 3.18	.732	28.28 ± 6.18	23.10 ± 7.38	.042*	27.14 ± 6.19	.004*	20.86 ± 7.15	< .001*	1.14 ± 2.17	2.24 ± 2.60	.057	.045*	.001*
AVL at 4 mm to the apex (mm^3)	22.75 ± 4.83	20.93 ± 8.48	.477	20.13 ± 5.13	< .001*	17.98 ± 7.81	< .001*	2.62 ± 2.09	2.96 ± 2.54	.640	24.36 ± 4.34	22.51 ± 8.41	.457	23.25 ± 4.64	.002*	20.51 ± 7.81	< .001*	1.11 ± 1.99	2.00 ± 1.65	.079	.026*	.003*
AVL at 2 mm to the apex (mm^3)	6.01 ± 1.73	5.70 ± 2.43	.675	4.69 ± 2.07	< .001*	3.90 ± 2.47	< .001*	1.33 ± 1.04	1.80 ± 1.49	.265	6.79 ± 1.35	6.57 ± 2.76	.789	5.96 ± 1.69	<.001*	4.90 ± 2.49	< .001*	0.83 ± 0.99	1.67 ± 1.21	.020*	.104	.323
AVL at 1 mm to the apex (mm^3)	1.66 ± 0.67	1.49 ± 0.68	.430	1.05 ± 0.86	< .001*	0.71 ± 0.81	< .001*	0.61 ± 0.63	0.79 ± 0.72	.400	1.96 ± 0.47	1.94 ± 0.86	.923	1.47 ± 0.73	< .001*	1.01 ± 0.82	< .001*	0.49 ± 0.51	0.93 ± 0.73	.040*	.388	.011*
Incisor with more resorption																						
Root length (mm)	15.00	11.95		13.79		10.40		1.21	1.55		13.90	13.94		13.20		12.24		0.70	1.70			
Root volume (mm^3)	290.05	179.32		256.81		164.16		33.24	15.16		266.06	192.93		239.21		176.76		26.85	16.16			
Cervical 1/3 volume (mm^3)	134.44	99.67		119.28		92.61		15.16	7.05		131.66	88.58		117.87		83.50		13.79	5.09			
Middle 1/3 volume (mm^3)	99.90	77.80		71.64		54.02		28.26	23.78		95.27	82.71		86.05		75.80		9.23	6.91			

(*continued on next page*)

Table 2 (*continued*)

	Manual							AI							Manual vs AI		
	T0 (Baseline)			T1 (141.9 ±. 4.9)			T0-T1	T0 (Baseline)			T1 (141.9 ±. 4.9)			T0-T1			T0-T1	
	Control ($n = 36$)	Experimental ($n = 33$)		Control ($n = 36$)		Experimental ($n = 33$)		Control ($n = 36$)	Experimental ($n = 33$)		Control ($n = 36$)		Experimental ($n = 33$)		Control ($n = 36$)	Experimental ($n = 33$)		Control ($n = 36$)	Experimental ($n = 33$)
	Mean ± SD	Mean ± SD	*P* value	Mean ± SD	*P* value	Mean ± SD	*P* value	Mean ± SD	Mean ± SD	*P* value	Mean ± SD	*P* value	Mean ± SD	*P* value	Mean ± SD	Mean ± SD	*P* value	*P* value	*P* value
Apical 1/3 volume (mm ^{3}) (AVL)	31.65	41.58		22.04		27.18		9.61	14.41		25.43	29.92		19.13		16.12		6.30	13.80			
AVL at 4 mm to the apex (mm^3)	19.00	24.93		11.33		15.96		7.68	8.98		19.21	36.27		13.62		29.19		5.59	7.07			
AVL at 2 mm to the apex (mm^3)	3.77	7.15		0.60		1.54		3.17	5.62		5.19	9.38		2.18		5.61		3.01	3.77			
AVL at 1 mm to the apex (mm^3)	2.37	2.52		0.66		0.20		1.72	2.33		1.46	3.77		0.12		1.30		1.34	2.47			
Central incisor	($n = 18$)	($n = 18$)		($n = 18$)		($n = 18$)		($n = 18$)	($n = 18$)		($n = 18$)	($n = 18$)		($n = 18$)		($n = 18$)		($n = 18$)	($n = 18$)			
Root length (mm)	13.44 ± 1.05	12.38 ± 1.58		13.22 ± 1.08		11.89 ± 1.75		0.22 ± 0.03	0.49 ± 0.17		13.15 ± 1.01	12.05 ± 1.64		12.97 ± 1.03		11.66 ± 1.74		0.18 ± 0.02	0.39 ± 0.11			
Root volume (mm^3)	242.62 ± 34.65	198.20 ± 43.07		232.96 ± 31.76		191.36 ± 43.88		9.66 ± 2.89	6.84 ± 0.81		241.74 ± 33.08	197.39 ± 43.65		238.74 ± 32.69		194.31 ± 43.95		3.01 ± 0.39	3.08 ± 0.30			
Cervical 1/3 volume (mm^3)	127.05 ± 16.62	108.40 ± 22.73		123.90 ± 15.94		106.87 ± 23.31		3.15 ± 0.68	1.52 ± 0.58		125.49 ± 15.88	107.16 ± 23.94		124.71 ± 16.86		107.10 ± 23.83		0.77 ± 0.97	0.06 ± 0.11			
Middle 1/3 volume (mm^3)	84.06 ± 13.30	66.67 ± 16.01		80.52 ± 11.72		64.51 ± 16.10		3.55 ± 1.58	2.16 ± 0.09		84.06 ± 12.16	66.25 ± 15.29		82.97 ± 11.79		65.34 ± 15.15		1.10 ± 0.38	0.91 ± 0.14			
Apical 1/3 volume (mm^3) (AVL)	31.51 ± 6.78	23.14 ± 7.86		28.53 ± 6.28		19.97 ± 7.06		2.98 ± 0.50	3.16 ± 0.80		32.20 ± 5.69	23.99 ± 7.58		31.07 ± 5.27		21.32 ± 7.29		1.12 ± 0.42	2.67 ± 0.29			
AVL at 4 mm to the apex (mm^3)	25.35 ± 4.75	22.54 ± 9.33		22.76 ± 4.98		19.20 ± 8.21		2.59 ± 0.24	3.34 ± 1.12		27.16 ± 3.84	24.44 ± 9.00		26.05 ± 3.91		22.22 ± 7.98		1.11 ± 0.07	2.22 ± 1.02			
AVL at 2 mm to the apex (mm^3)	6.56 ± 1.90	5.80 ± 2.43		5.47 ± 2.14		3.94 ± 2.27		1.09 ± 0.23	1.86 ± 0.16		7.47 ± 1.34	7.01 ± 2.92		6.66 ± 1.46		5.17 ± 2.37		0.81 ± 0.13	1.83 ± 0.55			

(*continued on next page*)

Table 2 (*continued*)

	Manual							AI							Manual vs AI	
	T0 (Baseline)			T1 (141.9 ±. 4.9)			T0-T1			T0 (Baseline)			T1 (141.9 ±. 4.9)			T0-T1			T0-T1	
	Control ($n = 36$)	Experimental ($n = 33$)		Control ($n = 36$)	Experimental ($n = 33$)		Control ($n = 36$)	Experimental ($n = 33$)		Control ($n = 36$)	Experimental ($n = 33$)		Control ($n = 36$)	Experimental ($n = 33$)		Control ($n = 36$)	Experimental ($n = 33$)		Control ($n = 36$)	Experimental ($n = 33$)
	Mean ± SD	Mean ± SD	*P* value	Mean ± SD	Mean ± SD	*P* value	Mean ± SD	Mean ± SD	*P* value	Mean ± SD	Mean ± SD	*P* value	Mean ± SD	Mean ± SD	*P* value	Mean ± SD	Mean ± SD	*P* value	*P* value	*P* value
AVL at 1 mm to the apex (mm^3)	1.84 ± 0.71	1.50 ± 0.67		1.38 ± 0.89	0.62 ± 0.67		0.46 ± 0.18	0.88 ± 0.00		2.17 ± 0.49	2.10 ± 0.96		1.69 ± 0.62	1.04 ± 0.74		0.49 ± 0.14	1.06 ± 0.22			
Lateral incisor	($n = 18$)	($n = 15$)		($n = 18$)	($n = 15$)		($n = 18$)	($n = 15$)		($n = 18$)	($n = 15$)		($n = 18$)	($n = 15$)		($n = 18$)	($n = 15$)			
Root length (mm)	13.20 ± 0.75	12.85 ± 1.92		12.82 ± 0.85	12.45 ± 1.96		0.37 ± 0.10	0.40 ± 0.04		12.82 ± 0.81	12.68 ± 1.86		12.60 ± 0.85	12.23 ± 1.90		0.22 ± 0.04	0.46 ± 0.04			
Root volume (mm^3)	174.19 ± 18.99	161.51 ± 45.39		167.41 ± 20.68	156.41 ± 44.27		6.78 ± 1.69	5.10 ± 1.11		169.78 ± 21.34	164.10 ± 45.99		167.91 ± 21.61	162.47 ± 47.25		1.87 ± 0.27	1.63 ± 1.26			
Cervical 1/3 volume (mm^3)	88.38 ± 9.29	85.65 ± 23.14		86.72 ± 10.47	83.98 ± 22.62		1.66 ± 1.18	1.67 ± 0.51		85.50 ± 10.40	86.13 ± 23.19		85.02 ± 11.06	85.67 ± 23.46		0.49 ± 0.66	0.46 ± 0.26			
Middle 1/3 volume (mm^3)	63.23 ± 11.31	56.19 ± 17.55		59.17 ± 7.65	53.86 ± 16.79		4.07 ± 3.66	2.34 ± 0.75		59.92 ± 8.03	55.90 ± 16.77		59.69 ± 7.89	56.44 ± 17.82		0.24 ± 0.14	−0.54 ± 1.05			
Apical 1/3 volume (mm^3) (AVL)	24.08 ± 3.84	21.81 ± 8.39		21.23 ± 4.58	18.57 ± 5.98		2.86 ± 0.74	3.23 ± 2.41		24.36 ± 3.71	22.04 ± 7.24		23.20 ± 4.29	20.31 ± 7.19		1.15 ± 0.58	1.74 ± 0.05			
AVL at 4 mm to the apex (mm^3)	20.16 ± 3.35	19.01 ± 7.18		17.51 ± 3.86	16.51 ± 7.31		2.64 ± 0.51	2.50 ± 0.13		21.56 ± 2.73	20.20 ± 7.27		20.45 ± 3.54	18.46 ± 7.35		1.11 ± 0.81	1.74 ± 0.08			
AVL at 2 mm to the apex (mm^3)	5.47 ± 1.38	5.57 ± 2.52		3.90 ± 1.73	3.85 ± 2.77		1.57 ± 0.35	1.73 ± 0.26		6.10 ± 0.99	6.05 ± 2.55		5.26 ± 1.65	4.58 ± 2.67		0.85 ± 0.65	1.47 ± 0.13			
AVL at 1 mm to the apex (mm^3)	1.48 ± 0.59	1.48 ± 0.71		0.72 ± 0.71	0.81 ± 0.96		0.76 ± 0.13	0.68 ± 0.26		1.76 ± 0.36	1.75 ± 0.71		1.26 ± 0.79	0.99 ± 0.92		0.50 ± 0.43	0.76 ± 0.21			

*: $P < .05$=statistically significant.

Table 3. Multiple linear regression predicting the amount of root resorption.

		Manual Segmentation								AI Segmentation			
		Simple model				Multiple model				Simple model			
	Category	Regression coefficient	IC 95% min—max		*P* value	Regression coefficient	IC 95% min—max		*P* value	Regression coefficient	IC 95% min—max		*P* value
Group	Control	0	-	-	-					0	-	-	-
Root length	Experimental	0.15	−0.13	0.43	.303	0.15	−0.11	0.41	.260	0.22	−0.01	0.45	.060
Root Volume	Experimental	−2.17	−6.65	2.31	.343	−0.34	−4.21	3.53	.863	−0.02	−3.94	3.89	.992
Cervical 1/3 volume	Experimental	−0.82	−3.21	1.58	.504	−1.06	−3.02	0.90	.290	−0.39	−2.49	1.71	.718
Middle 1/3 volume	Experimental	−1.57	−4.04	0.91	.216	−0.62	−3.38	2.13	.658	−0.42	−2.07	1.24	.624
Apical 1/3 volume	Experimental	0.28	−1.31	1.87	.732	1.10	−0.38	2.58	.144	1.11	−0.03	2.25	.057
AVL at 4 mm to the apex	Experimental	0.34	−1.09	1.77	.640	0.89	−0.51	2.29	.211	0.89	−0.10	1.88	.079
AVL at 2 mm to the apex	Experimental	0.47	−0.36	1.31	.265	0.48	−0.27	1.24	.209	0.84	0.13	0.55	**.020***
AVL at 1 mm to the apex	Experimental	0.18	−0.24	0.60	.400	0.19	−0.19	0.57	.333	0.43	0.02	0.85	**.040***
Gender	Male	0	-	-	-								
Root length	Female	0.00	−0.25	0.26	.986					0.06	−0.16	0.28	.605
Root Volume	Female	2.15	−2.69	6.99	.384					−2.34	−6.72	2.04	.295
Cervical 1/3 volume	Female	2.56	0.21	4.90	**.033***	2.10	0.09	4.11	**.041***	−0.56	−3.00	1.88	.654

(*continued on next page*)

Table 3 (*continued*)

		Manual Segmentation								AI Segmentation			
		Simple model				Multiple model				Simple model			
	Category	Regression coefficient	IC 95% min—max		*P* value	Regression coefficient	IC 95% min—max		*P* value	Regression coefficient	IC 95% min—max		*P* value
Middle 1/3 volume	Female	1.88	−0.48	4.25	.119					−0.95	−2.78	0.88	.309
Apical 1/3 volume	Female	−0.71	−2.33	0.91	.393					−0.58	−1.85	0.70	.375
AVL at 4 mm to the apex	Female	−0.95	−2.43	0.54	.213					−0.82	−1.97	0.32	.157
AVL at 2 mm to the apex	Female	−0.43	−1.30	0.44	.331					−0.44	−1.27	0.40	.305
AVL at 1 mm to the apex	Female	−0.27	−0.70	0.15	.203					−0.25	−0.73	0.23	.309
Age													
Root length		0.00	−0.01	0.01	.686					−0.01	−0.01	0.00	**.041***
Root Volume		−0.02	−0.17	0.14	.839					0.05	−0.12	0.21	.590
Cervical 1/3 volume		−0.07	−0.15	0.01	.084	−0.05	−0.12	0.02	.167	0.03	−0.05	0.10	.506
Middle 1/3 volume		0.01	−0.06	0.08	.745					0.03	−0.03	0.10	.294
Apical 1/3 volume		0.02	−0.02	0.06	.413					−0.01	−0.06	0.04	.683
AVL at 4 mm to the apex		0.03	−0.01	0.07	.174					−0.01	−0.06	0.04	.648
AVL at 2 mm to the apex		0.01	−0.01	0.03	.457					−0.01	−0.03	0.02	.530
AVL at 1 mm to the apex		0.01	−0.01	0.02	.206					−0.01	−0.02	0.01	.631
Malocclusion	Class I	0	-	-	-					0	-	-	-

(*continued on next page*)

Table 3 (*continued*)

		Manual Segmentation								AI Segmentation			
		Simple model				Multiple model				Simple model			
	Category	Regression coefficient	IC 95% min—max		*P* value	Regression coefficient	IC 95% min—max		*P* value	Regression coefficient	IC 95% min—max		*P* value
Root length					**.020***				**.008****				.700
	Class II	0.05	−0.24	0.34	.742	0.04	−0.23	0.31	.752	0.06	−0.16	0.29	.589
	Class III	−0.20	−0.41	0.01	.060	−0.21	−0.40	−0.02	**.032***	−0.02	−0.12	0.08	.727
Root Volume					.406								.850
	Class II	1.79	−2.29	5.87	.389					0.59	−3.46	4.64	.775
	Class III	−1.91	−5.91	2.10	.350					1.90	−2.64	4.81	.568
Cervical 1/3 volume					.810								.825
	Class II	0.80	−1.81	3.40	.549					0.64	−1.53	2.80	.566
	Class III	0.17	−1.93	2.27	.876					0.37	−0.97	1.72	.588
Middle 1/3 volume					.142								.726
	Class II	1.77	−0.52	4.06	.130					0.25	−1.50	2.00	.781
	Class III	−0.93	−3.25	1.40	.434					0.77	−1.13	2.68	.427
Apical 1/3 volume					**.015***				.700				.997
	Class II	−1.34	−2.90	0.22	.093	−0.06	−1.61	1.50	.943	−0.02	−1.35	1.31	.973
	Class III	0.52	−1.18	2.22	.546	−0.46	−1.70	0.79	.474	−0.06	−1.58	1.47	.942
					.001**				.086				.807
AVL at 4 mm to the apex	Class II	0.06	−1.58	1.70	.942	−0.32	−1.95	1.30	.696	−0.43	−1.71	0.85	.514
	Class III	−1.67	−3.18	−0.16	**.030***	−1.10	−2.24	0.04	.058	−0.30	−1.82	1.23	.704

(*continued on next page*)

Table 3 (*continued*)

		Manual Segmentation								AI Segmentation			
		Simple model				Multiple model				Simple model			
	Category	Regression coefficient	IC 95% min—max		*P* value	Regression coefficient	IC 95% min—max		*P* value	Regression coefficient	IC 95% min—max		*P* value
AVL at 2 mm to the apex					<.001***				.001**				.570
	Class II	0.06	−0.94	1.05	.914	0.04	−0.87	0.95	.933	−0.27	−1.19	0.65	.567
	Class III	−1.00	−1.87	−0.12	.026*	−1.02	−1.89	−0.15	.021*	−0.48	−1.40	0.43	.302
AVL at 1 mm to the apex					<.001***				<.001***				.362
	Class II	−0.04	−0.55	0.48	.894	−0.04	−0.51	0.43	.866	−0.15	−0.66	0.37	.581
	Class III	−0.53	−0.99	−0.07	.023*	−0.54	−0.98	−0.11	.015*	−0.32	−0.80	1.66	.197
Treatment duration													
Root length		0.01	−0.02	0.04	.447					0.02	−0.01	0.04	.315
Root Volume		−0.47	−0.88	−0.06	.025*	−0.45	−0.83	−0.08	.018*	−0.32	−0.83	0.19	.214
Cervical 1/3 volume		−0.14	−0.33	0.05	.148					−0.17	−0.49	0.16	.318
Middle 1/3 volume		−0.26	−0.40	−0.12	<.001***	−0.23	−0.42	−0.05	.015*	−0.13	−0.32	0.07	.211
Apical 1/3 volume		−0.17	−0.27	−0.06	.001**	−0.20	−0.33	−0.07	.002**	−0.04	−0.11	0.02	.212
AVL at 4 mm to the apex		−0.11	−0.21	−0.02	.023*	−0.13	−0.26	−0.01	.047*	−0.03	−0.09	0.03	.346
AVL at 2 mm to the apex		−0.03	−0.09	0.03	.362					0.01	−0.07	0.08	.842
AVL at 1 mm to the apex		−0.01	0.03	0.03	.649					0.01	−0.04	0.06	.676

[a]Dependent variable: root volume change.
*: $P < .045$, **: $P < .01$, ***: $P < .001$.

the global level, volume by thirds, and 4 mm from the apex. However, as we approached apically, the differences equalized and even diminished, resulting in a greater loss with automatic segmentation 1 mm from the apex in the EG ($P = .011$) (Table 2).

Length loss showed similar changes in both manual and automatic segmentations ($P > .05$).

DISCUSSION

The aim of the present study was to compare the short-term impact of two different orthodontic force magnitude regimes on EARR. Additionally, two different 3D volumetric quantification methods were analyzed: manual and automated segmentation. Differences were observed between multiforce archwires that applied customized forces to the teeth and the conventional Ni-Ti archwire sequence. Moreover, the manual and automated segmentation methods presented the same tendency of change in both groups, with a slightly greater volume loss observed with manual segmentation; however, as we moved apically, the volume loss was greater with automatic segmentation.

Although 3D imaging is considered an indispensable tool in digital dentistry,[34,35,41] limited studies have provided volumetric results for root resorption using CBCT.[14,15,42,43] This suggests the scarcity of scientific evidence on this subject.

The optimal physiological magnitude and regime of clinically useful orthodontic forces remain undefined, although the results described in the literature are controversial.[2] Numerous *in vivo* studies using animal models have been conducted to ascertain the effects of orthodontic tooth movement and the magnitude of the force applied.[44] In addition, experimental studies have used different archwires to analyze the force applied during the initial treatment months.[45,46] In terms of root resorption, intermittent forces are less harmful to root structural integrity than continuous forces.[22,47,48] However, fixed orthodontic appliances deliver a constant force along the arch through archwires.

Some studies have assessed the clinical effectiveness and impact of archwires used in the alignment phase on EARR.[3,49-52] Nevertheless, the impact analysis and the effect on the roots consist of 2D records, which are limited in terms of the accuracy of the magnitude of root resorption. The present randomized clinical trial provides novel data on the impact of the differential magnitudes of orthodontic forces on root integrity using high-precision 3D volumetric analysis. Interestingly, contrary to what has been hypothesized, the results of the present study indicate that the force magnitude itself during the initial stages of treatment might not be a critical factor that promotes EARR. Instead, the distribution pattern of this magnitude of forces in different regions of the root structure may have a critical impact on EARR. It seems plausible that multiforce archwire sequences, although delivering individualized low force magnitudes (50gr vs 100gr or more delivered in the same upper incisor region through conventional arches), might induce higher stress to the apical part of the root and, therefore, lead to greater root loss. These findings are consistent with the results of recent investigations on the force delivered by multiforce archwires.[25] In this respect, this study highlights the importance of factors dependent on the wire cross-section and dimensions and concludes that multiforce wires might exceed the range of ideal forces in certain circumstances during the initial phases of treatment owing to the type of square and rectangular sections and the force and moments generated in the slot (moment of inertia, I).

In line with this, at initial treatment stages, teeth are more likely to be misaligned with each other; therefore, the bends of the arch between adjacent brackets increase with forces and force couples applied in all three directions. If a wire is to be bent in many directions, it should be able to slide easily through the slots of the brackets, because at this stage, it is desirable that almost all the force of the arch be directed toward the dental movement.[53] When an archwire contacts the edges of the bracket slot during tipping, the geometry and material properties of the wire govern the wireś ability to bend in the slot. Therefore, small flexible archwires, which provide more clearance between the wire and the walls of the bracketś slot, require less force to slide a bracket than that of a larger one.[54,55] Therefore, the size and shape of the archwire play an important role in the resistance to sliding. As extrapolated to the present research, the diameter of the initial archwires included in the sequence of the EG group (0.018 × 0.018-inch followed by a 0.016 × 0.022-inch Ni-Ti) exerted a much lower force (estimated at 50 and 80gr of force, respectively, at the upper incisors) than the gold standard archwire of 0.014-inch (estimated at 100gr of force at the upper incisors). The frictional component of the archwire-bracket couple, as well as forces and moments exerted in the EG group, might have induced a higher stress to the apical third of the tooth root, resulting in a high apical root volume loss in the group undergoing lower force magnitude (2.24 ± 2.60 mm^3 and 1.14 ± 2.17 mm^3 in the EG and CG groups, respectively; this especially occurred in the apical third region at 1 and 2 mm from the root apex; Table 2).

Interestingly, this effect on root volume loss was not observed in the more coronally displaced regions, where no statistically significant differences were observed between the higher- and lower-force groups. Hence, such differences retrieved no statistical differences when AI-aided segmentation was performed; this highlights the effects of the 3D volumetric assessment method. Preliminary results of the present RCT revealed that the individualized force magnitude delivered by the personalized force archwire sequence showed no superiority in terms of root resorption prevention com-

pared to the standard of care with the conventional superelastic archwire sequence.

As a secondary outcome, the present study aimed to provide a deep comparison between a more traditional manual tooth segmentation method and a novel automatic AI-aided segmentation approach.[32,38-40] Manual segmentation is laborious, expensive, and time-consuming. AI segmentation took less than 60 s to segment a full set of teeth and roots on the DICOM file of CBCT, compared to a mean of 5 h with manual segmentation.[32,34,35,41] To date, the present study is the first to compare the conventional manual process of segmentation with a fully automated approach, with the aim of analyzing root volume loss using multiforce zone archwires. The results showed a significantly greater generalized loss of root volume (both total and analyzed by thirds) with manual segmentation than with automated segmentation. A possible explanation could be the influence of the observer performance during manual segmentation or the lower accuracy of the AI methods. Unlike AI, human contributions might unintentionally alter the measurement, particularly during the second CBCT (T1), where the presence of braces may unconsciously affect the details of the final segmentation. In addition, the high density of the braces in T1 records must be taken into account, which produces a clear image distortion that may contribute to different quantification of the average volume with any method of measurement. Nevertheless, no differences were found in *root length loss* between the two segmentations. In addition, as the measurement moves toward the root apex, these differences diminish until the situation reverses, with the AI segmentation method ultimately showing a slightly increased *volume loss* at 1 mm from the apex. It is also interesting to note that both groups (CG and EG) were fairly homogeneous at the beginning of treatment in all variables, except for the volume of the middle and apical 1/3. The CG showed a larger root volume in these regions, as detected using manual and AI segmentations. This demonstrates that the trend of changes with both types of segmentation closely resembles each other; therefore, we can ensure high accuracy and reliability of both segmentation methods.

A previously published analysis of root volume [41] showed that after automatically segmenting the teeth, the authors divided crowns from roots with a pre-established cutting plane defined by a normal average crown length reported in the literature. Subsequently, the crowns of each tooth were superimposed at different time points, and the volumetric changes were calculated from the reference plane to the root apex. In the present study, the reference plane was manually defined on the cementoenamel junction of each tooth. This individualization was undertaken because of the variability in crown size of the general population,[56] as well as the influence of crown changes due to attrition or any other anomaly, which could easily alter the precision of the method. Importantly, as previously noted, current manual tooth segmentation methods have certain disadvantages, such as time consumption and the influence of the clinicianś experience on the process. AI-based and custom-made automated segmentation methods have been developed to overcome the disadvantages associated with the current 2D and manual 3D methodologies.[35,41] However, none of the previously published automated approaches have reported the possibility of manual correction after automated segmentation. Despite the high precision and low time consumption of AI, daily clinical practice often presents with challenging situations. In cases with low-exposure CBCT and a limited definition, the accuracy of tooth segmentation may be inadequate, forcing the recording to be discarded. With manual intervention, which is time-consuming, a more careful segmentation of these types of records can be successfully performed. Another consideration is the need for larger sample size to account for the results influenced by confounding factors (sex, age, type of malocclusion, and treatment duration). Furthermore, despite employing rigorous methodology for randomization and allocation concealment to mitigate bias, it was challenging to blind both the clinician to the allocation group and the investigator to CBCT segmentation.

CONCLUSIONS

- Preliminary results of the present RCT revealed that the individualized force magnitude delivered by the multiforce archwire sequence showed no superiority in terms of root resorption prevention compared with the standard of care through the conventional Ni-Ti archwire sequence.
- The present study provides a clinically useful method for volumetric root resorption quantification aided by AI, which retrieves results similar to those obtained by manual segmentation.
- This study suggests the positive impact of implementing AI technology in the field of dentistry in general and tooth segmentation in particular. High accuracy and especially low time consumption, which simplifies the existing digital workflow of orthodontics and general dentistry, were highlighted. This will enhance the treatment outcomes and further improve the level of evidence.

ETHICS APPROVAL AND CONSENT TO PARTICIPATE

This study was conducted in accordance with the ethical standards of the institutional and national research committee. Ethical approval was granted by the San Carlos Hospital Ethical Review Board, approval number 21/003-EC_P and the Local Review Board (*URI+i: 51-100521*). All participants and, where applicable, their legal guardians, were informed about the nature of the research and its objectives.

AVAILABILITY OF DATA AND MATERIAL

The datasets used and/or analyzed during the current study are available from the Corresponding Author on reasonable request.

ACKNOWLEDGMENTS

The authors wish to thank Dr Teresa Baena de la Iglesia as expert researcher during calibration for the training and calibration test periods.

CREDIT AUTHORSHIP CONTRIBUTION STATEMENT

NAVARRO-FRAILE ESTRELLA: Writing – original draft, Conceptualization. **DEHESA-SANTOS ALEXANDRA:** Writing – original draft. **CHEN YUN:** Writing – original draft. **JUAN CARLOS PALMA-FERNÁNDEZ:** Writing – original draft. **IGLESIAS-LINARES ALEJANDRO:** Methodology, Conceptualization.

SUPPLEMENTARY MATERIALS

Supplementary material associated with this article can be found, in the online version, at doi:10.1016/j.jebdp.2025.102095.

REFERENCES

1. Sharab LY, Morford LA, Dempsey J, et al. Genetic and treatment-related risk factors associated with external apical root resorption (EARR) concurrent with orthodontia. *Orthod Craniofacial Res.*. 2015;18(S1):71–82.
2. Roscoe MG, Meira JBC, Cattaneo PM. Association of orthodontic force system and root resorption: a systematic review. *Am J Orthod Dentofac.* 2015;147(5):610–626.
3. Phermsang-ngarm P, Charoemratrote C. Tooth and bone changes after initial anterior dental alignment using preformed vs customized nickel titanium archwires in adults: a randomized clinical trial. *Angle Orthod.* 2018;88(4):425–434.
4. PEREIRA ABN, ALMEIDA R, ARTESE F, DARDENGO C, QUINTÃO C, CARVALHO F. External root resorption evaluated by CBCT 3D models superimposition. *Dent Press J Orthod.*. 2022;27(02):e2219315.
5. Alzahawi K, Færøvig E, Brudvik P, Bøe OE, Mavragani M. Root resorption after leveling with super-elastic and conventional steel arch wires: a prospective study. *Prog Orthod.* 2014;15(1):35.
6. LNU J, Singh S, Adarsh K, Kumar A, Gupta AR, Sinha A. Comparison of apical root resorption in patients treated with fixed orthodontic appliance and clear aligners: a cone-beam computed tomography study. *J Contemp Dent Pract.* 2021;22(7):763–768.
7. Surya S, Barua AND, Magar SP, Magar SS, Rela R, Chhabada AK. Comparative assessment of the efficacy of two-dimensional digital intraoral radiography to three-dimensional cone beam computed tomography in the diagnosis of periapical pathologies. *J Pharm Bioallied Sci.* 2022;14(Suppl 1):S1009–S1013.
8. Iglesia TB la, Yañez-Vico RM, Iglesias-Linares A. Diagnostic performance of cone-beam computed tomography to diagnose in vivo/in vitro root resorption: a systematic review and meta-analysis. *J Évid-Based Dent Pr.* 2023;23(1):101803.
9. Lund H, Gröndahl K, Gröndahl H-G. Cone beam computed tomography for assessment of root length and marginal bone level during orthodontic treatment. *Angle Orthod.* 2010;80(3):466–473.
10. Johansson K, Lindh C, Paulsson L, Rohlin M. A tool for assessment of risk of bias in studies of adverse effects of orthodontic treatment applied in a systematic review on external root resorption. *Eur J Orthodont.* 2020;43(4):457–466.
11. Chen J, Ning R. Evaluation of root resorption in the lower incisors after orthodontic treatment of skeletal class III malocclusion by three-dimensional volumetric measurement with cone-beam computed tomography. *Angle Orthod.* 2023;93:320–327.
12. Wan J, Zhou S, Wang J, Zhang R. Three-dimensional analysis of root changes after orthodontic treatment for patients at different stages of root development. *Am J Orthod Dentofac.* 2023;163(1):60–67.
13. Liu W, Shao J, Li S, et al. Volumetric cone-beam computed tomography evaluation and risk factor analysis of external apical root resorption with clear aligner therapy. *Angle Orthod.* 2021;91(5):597–603.
14. Aras I, Unal I, Huniler G, Aras A. Root resorption due to orthodontic treatment using self-ligating and conventional brackets. *J Orofac Orthop Fortschritte Der Kieferorthopädie.* 2018;79(3):181–190.
15. Puttaravuttiporn P, Wongsuwanlert M, Charoemratrote C, Leethanakul C. Volumetric evaluation of root resorption on the upper incisors using cone beam computed tomography after 1 year of orthodontic treatment in adult patients with marginal bone loss. *Angle Orthod.* 2018;88(6):710–718.
16. Arvind TRP, Ramasamy N, Subramanian AK, Selvaraj A, Siva S. Three-dimensional volumetric evaluation of root resorption in maxillary anteriors following en-masse retraction with varying force vectors – a randomized control trial. *Orthod Craniofacial Res.* 2024;27(2):211–219.
17. Gandhi V, Mehta S, Gauthier M, et al. Comparison of external apical root resorption with clear aligners and pre-adjusted edgewise appliances in non-extraction cases: a systematic review and meta-analysis. *Eur J Orthodont.* 2020;43(1):15–24.
18. Dao V, Mallya SM, Markovic D, Tetradis S, Chugal N. Prevalence and characteristics of root resorption identified in cone-beam computed tomography scans. *J Endodont.* 2023;49(2):144–154.
19. Futyma-Gąbka K, Różyło-Kalinowska I, Piskórz M, Bis E, Borek W. Evaluation of root resorption in maxillary ante-

rior teeth during orthodontic treatment with a fixed appliance based on panoramic radiographs. *Pol J Radiol*. 2022;87(1):e545–e548.

20. Wang J, Lamani E, Christou T, Li P, Kau CH. A randomized trial on the effects of root resorption after orthodontic treatment using pulsating force. *BMC Oral Health*. 2020;20(1):238.
21. Theodorou CI, Kuijpers-Jagtman AM, Bronkhorst EM, Wagener FADTG. Optimal force magnitude for bodily orthodontic tooth movement with fixed appliances: a systematic review. *Am J Orthod Dentofac*. 2019;156(5):582–592.
22. Currell SD, Liaw A, Grant PDB, Esterman A, Nimmo A. Orthodontic mechanotherapies and their influence on external root resorption: a systematic review. *Am J Orthod Dentofac*. 2019;155(3):313–329.
23. Smale I, Årtun J, Behbehani F, Doppel D, van't Hof M, Kuijpers-Jagtman AM. Apical root resorption 6 months after initiation of fixed orthodontic appliance therapy. *Am J Orthod Dentofac*. 2005;128(1):57–67.
24. Artun J, Smale I, Behbehani F, Doppel D, Hof MV, Kuijpers–Jagtman AM. Apical root resorption six and 12 months after initiation of fixed orthodontic appliance therapy. *Angle Orthod*. 2005;75(6):919–926.
25. Sanders E, Johannessen L, Nadal J, Jäger A, Bourauel C. Comparison of multiforce nickel–titanium wires to multistrand wires without force zones in bending and torque measurements. *J Orofac Orthop Fortschritte Kieferorthopädie*. 2022;83(6):382–394.
26. Stoyanova-Ivanova A, Georgieva M, Petrov V, Andreeva L, Petkov A, Georgiev V. Effects of clinical use on the mechanical properties of Bio-Active® (BA) and TriTanium® (TR) multiforce nickel-titanium orthodontic archwires. *Materials*. 2023;16(2):483.
27. Stoyanova-Ivanova A, Georgieva M, Petrov V, et al. Thermal behavior changes of as-received and retrieved Bio-Active® (BA) and TriTanium® (TR) multiforce nickel–titanium orthodontic archwires. *Materials*. 2023;16(10):3776.
28. Olsen ME. SmartArch multi-force superelastic archwires: a new paradigm in orthodontic treatment efficiency. *J Clin Orthod: JCO*. 2020;54(2):70–81.
29. Lombardo L, Ceci M, Mollica F, Mazzanti V, Palone M, Siciliani G. Mechanical properties of multi-force vs. conventional NiTi archwires. *J Orofac Orthop Fortschritte Kieferorthopädie*. 2019;80(2):57–67.
30. Ibe DM, Segner D. Superelastic materials displaying different force levels within one archwire. *J Orofac Orthop Fortschritte Kieferorthopädie*. 1998;59(1):29–38.
31. Dudic A, Giannopoulou C, Leuzinger M, Kiliaridis S. Detection of apical root resorption after orthodontic treatment by using panoramic radiography and cone-beam computed tomography of super-high resolution. *J Orofac Orthop Dentofac Orthop*. 2009;135(4):434–437.
32. Wang H, Minnema J, Batenburg KJ, Forouzanfar T, Hu FJ, Wu G. Multiclass CBCT image segmentation for orthodontics with deep learning. *J Dent Res*. 2021;100(9):943–949.
33. Joda T, Bornstein MM, Jung RE, Ferrari M, Waltimo T, Zitzmann NU. Recent trends and future direction of dental research in the digital era. *Int J Environ Res Public Heal*. 2020;17(6):1987.
34. Lahoud P, EzEldeen M, Beznik T, et al. Artificial intelligence for fast and accurate 3-dimensional tooth segmentation on cone-beam computed tomography. *J Endodont*. 2021;47(5):827–835.
35. Shaheen E, Leite A, Alqahtani KA, et al. A novel deep learning system for multi-class tooth segmentation and classification on cone beam computed tomography. A validation study. *J Dent*. 2021;115:103865.
36. Preda F, Morgan N, Gerven AV, et al. Deep convolutional neural network-based automated segmentation of the maxillofacial complex from cone-beam computed tomography:a validation study. *J Dent*. 2022;124:104238.
37. Ren R, Luo H, Su C, Yao Y, Liao W. Machine learning in dental, oral and craniofacial imaging: a review of recent progress. *PeerJ*. 2021;9:e11451.
38. AnonWorld medical association declaration of Helsinki: ethical principles for medical research involving human subjects. *J Korean Med Assoc*. 2014;57(11):899–902.
39. Navarro-Fraile E, Dehesa-Santos A, Chen Y, Palma-Fernández JC, Iglesias-Linares A. Impact of force magnitude on volumetric root resorption: a two arms-parallel, randomized controlled clinical trial; preliminary results. Annual Congress of the European Orthodontic Society (EOS), "personal communication".
40. Lazcano-Ponce E, Salazar-Martínez E, Gutiérrez-Castrellón P, Angeles-Llerenas A, Hernández-Garduño A, Viramontes JL. Ensayos clínicos aleatorizados: variantes, métodos de aleatorización, análisis, consideraciones éticas y regulación. *Salud Pública De México*. 2004;46(6):559–584.
41. Alqahtani KA, Jacobs R, Shujaat S, Politis C, Shaheen E. Automated three-dimensional quantification of external root resorption following combined orthodontic-orthognathic surgical treatment. A validation study. *J Stomatol Oral Maxillofac Surg*. 2023;124(1):101289.
42. Nasser AR, Sultan K, Hajeer MY, Hamadah O. Investigating the effectiveness of low-level laser in reducing root resorption of the upper incisors during intrusion movement using mini-implants in adult patients with deep overbite: a randomized controlled clinical trial. *Cureus*. 2023;15(2):e35381.
43. Rossi A, Lagravère-Vich M, Heo G, Major PW, El-Bialy T. An evaluation of root resorption associated with the use of photobiomodulation during orthodontic treatment with clear aligners: a retrospective cohort pilot study. *Angle Orthod*. 2024;94:294–302.
44. Leeuwen EV, Kuijpers-Jagtman A, Hoff JV den, Wagener F, Maltha J. Rate of orthodontic tooth movement after changing

the force magnitude: an experimental study in beagle dogs. *Orthod Craniofac Res*. 2010;13(4):238–245.

45. AnonConstant versus dissipating forces in orthodontics: the effect on initial tooth movement and root resorption. *Brit Dent J*. 2003;195(11):659.
46. Mandall N, Lowe C, Worthington H, et al. Which orthodontic archwire sequence? A randomized clinical trial. *Eur J Orthodont*. 2006;28(6):561–566.
47. Weltman B, Vig KWL, Fields HW, Shanker S, Kaizar EE. Root resorption associated with orthodontic tooth movement: a systematic review. *Am J Orthod Dentofac*. 2010;137(4):462–476.
48. Yassir YA, McIntyre GT, Bearn DR. Orthodontic treatment and root resorption: an overview of systematic reviews. *Eur J Orthodont*. 2020;43(4):442–456.
49. Noori RM, Yassir YA. Effectiveness of tubular coaxial nickel-titanium and copper nickel-titanium orthodontic aligning archwires: a randomized clinical trial. *Int Orthod*. 2023;21(4):100812.
50. Wang Y, Liu C, Jian F, et al. Initial arch wires used in orthodontic treatment with fixed appliances. *Cochrane Db Syst Rev*. 2018;2018(7):CD007859.
51. BHATIA NK, CHUGH VK, SHANKAR SP, et al. Alignment efficiency and three-dimensional assessment of root resorption after alignment with conventional and copper-nickel-titanium archwires: a randomized controlled trial. *Dent Press J Orthod*. 2023;28(06):e2323177.
52. Elhanouty MZ, Al-Nimri KS, Alomari SA. A comparison between two orthodontic archwire sequences in terms of speed of alignment and root resorption: a randomized controlled clinical trial. *Clin Oral Investig*. 2023;27:1–8.
53. Thorstenson GA, Kusy RP. Effect of archwire size and material on the resistance to sliding of self-ligating brackets with second-order angulation in the dry state. *Am J Orthod Dentofac Orthop*. 2002;122(3):295–305.
54. Kusy RP, Withley JQ. Assessment of second-order clearances between orthodontic archwires and bracket slots via the critical contact angle for binding. *Angle Orthod*. 1999;69(1):71–80.
55. Liu C, Wei Z, Jian F, et al. Initial arch wires used in orthodontic treatment with fixed appliances. *Cochrane Database Syst Rev*. 2024;2024(2):CD007859.
56. Johe RS, Steinhart T, Sado N, Greenberg B, Jing S. Intermaxillary tooth-size discrepancies in different sexes, malocclusion groups, and ethnicities. *Am J Orthod Dentofac Orthop*. 2010;138(5):599–607.